

# BGPR\_Reconstruct: A MATLAB<sup>®</sup> ray-tracing program for nonlinear inversion of first arrival travel time data from zero-offset borehole radar<sup>☆</sup>

Dale F. Rucker\*, Ty P.A. Ferré

*Department of Hydrology and Water Resources, University of Arizona, P.O. Box 210110, Tucson, AZ 85721, USA*

Received 17 September 2003; received in revised form 20 April 2004; accepted 1 May 2004

## Abstract

A MATLAB program was developed to invert first arrival travel time picks from zero offset profiling borehole ground penetrating radar traces to obtain the electromagnetic wave propagation velocities in soil. Zero-offset profiling refers to a mode of operation wherein the centers of the bistatic antennae being lowered to the same depth below ground for each measurement. The inversion uses a simulated annealing optimization routine, whereby the model attempts to reduce the root mean square error between the measured and modeled travel time by perturbing the velocity in a ray tracing routine. Measurement uncertainty is incorporated through the presentation of the ensemble mean and standard deviation from the results of a Monte Carlo simulation. The program features a pre-processor to modify or delete travel time information from the profile before inversion and post-processing through presentation of the ensemble statistics of the water contents inferred from the velocity profile. The program includes a novel application of a graphical user interface to animate the velocity fitting routine.

© 2004 Elsevier Ltd. All rights reserved.

*Keywords:* Simulated annealing; Optimization; Graphical user interface; Monte Carlo; Uncertainty

## 1. Introduction

Borehole ground penetrating radar (BGPR) is a high-frequency geophysical method used to profile the water content in the shallow subsurface. The instrumentation consists of a transmitting antenna and a receiving antenna placed in parallel boreholes. An electromagnetic (EM) wave is propagated between the antennae. A signal arriving as a function of time at a single depth is known as a radar trace. A stacked series of radar traces recorded at different depths form a radargram. Typically, it is assumed that all waves are direct (travel along

a straight line from the transmitter to the receiver). With this assumption, the first arrival travel time at each depth can be divided by the borehole separation to determine the direct wave travel time, which is then used to infer the relative apparent dielectric permittivity of the medium between the boreholes. The dielectric permittivity is then related to the water content through empirical relations (e.g. Topp et al., 1980), semi-empirical relations such as geometric models (Feng and Sen, 1985; Friedman, 1998), statistical models (Friedman, 1997), or theoretical models (Tabbagh et al., 2000).

Zero-offset profiling (ZOP) with BGPR involves lowering the antennae simultaneously such that their centers are at the same depth for each measurement. In the multi-offset gather (MOG) approach, the antennae centers are located at different depths, leading to a larger

<sup>☆</sup> Code on server at <http://www.iamg.org/CGEditor/index.htm>.

\*Corresponding author. Tel./fax: +1-520-722-5360.

E-mail address: [druck@hwr.arizona.edu](mailto:druck@hwr.arizona.edu) (D.F. Rucker).

number of measurements to form a two-dimensional transillumination of the subsurface. The number of measurements in a MOG makes the method impractical for monitoring highly transient events. Additionally, interpretation of the MOG requires full tomographic inversion. ZOP BGPR is much faster and interpretation of the measured travel times is much simpler.

Despite the advantages of ZOP BGPR for monitoring rapid events, (Rucker and Ferré, 2003, 2004b) have shown that correct interpretation can be difficult under some conditions. Specifically, if the antennae are located in a soil that has a relatively low EM propagation velocity and near a soil that has a higher velocity, then a critically refracted wave may arrive before a direct wave. When refraction occurs the travel path cannot be known without knowledge of both propagation velocities. Therefore, it is difficult to determine the EM propagation velocity associated with the first arriving travel times on the radargram. Critical refraction is particularly important near the ground surface, where the propagation velocity through air ( $v_{air}=0.3$  m/ns) is much higher than that through soil ( $v_{soil}=0.03$ – $0.17$  m/ns). However, the effects of refraction are also seen at the boundaries between soil layers and at wetting fronts (Rucker and Ferré, 2004b).

If refraction occurs, correct interpretation of the water content profile requires that: (1) direct arrivals be identified on the radargram; and (2) more complete analysis be applied to determine the propagation velocity associated with critically refracted first arrivals. Direct wave first arrivals can be interpreted using the standard approach described above. However, the inversion of propagation velocity from first arrival travel times is nonlinear and ill posed for a critically refracted wave (Rucker and Ferré, 2004a). Unfortunately, it is impossible to distinguish direct and critically refracted first arrivals from direct examination of a single radar trace. Rather, the entire radargram must be examined to identify direct and critically refracted waves. Critically refracted waves can be identified on a radargram because they exhibit linearly increasing or decreasing travel times with depth. A graphical approach can be used to identify regions with first arriving critical refractions and to determine the propagation velocity from the slope of the linearly changing travel times with depth (Rucker and Ferré, 2003.). All other travel time values, not exhibiting a linear change with depth, can be considered direct arrivals.

The graphical approach to interpreting the water content profile is time consuming, especially for large data sets. Moreover, the slope obtained from the graphical solution is based on at least three consecutive measurements. As a result, depth resolution is reduced in regions of critical refraction.

We have developed an automated routine for inversion of ZOP BGPR first arrival travel times. Rather than

identifying direct and critically refracted arrivals directly, an optimization algorithm finds the propagation velocity profile that results in the minimum error between the measured first arrival travel time profile and that determined through forward modeling of EM propagation velocity based on ray tracing. Development of the routine is described in three stages. First, we develop MATLAB ray tracing routines for predicting the first arrival travel time of EM waves including considerations of critical refraction. Second, we develop an optimization algorithm that identifies the propagation velocity profile that results in the minimum error between the measured and modeled measured first arrival travel time profiles. Third, we incorporate stochastic parameter estimation through Monte Carlo analysis to quantify the effects of uncertainties inherent in ZOP BGPR travel time measurements on the accuracy of inferred water content profiles (Rucker and Ferré, 2004a). The routine includes a MATLAB graphical user interface for ease of use.

## 2. Theory

### 2.1. Forward modeling of the first arrival time profile through ray tracing

The propagation of electromagnetic waves through low loss media is described by Maxwell's equations. Because these equations can be difficult to solve, both analytically and numerically, simple approximations are made to simulate waves as rays. Ray paths describe the directional path of a wave through a medium. In a perfect dielectric medium (electrical conductivity is zero), rays travel along straight lines through the medium with a constant dielectric permittivity and they reflect or refract at boundaries between media with different dielectric permittivities. It can be shown that reflected waves are never first arriving on a radar trace. Therefore, we only consider direct and refracted waves.

The travel time of a direct wave ( $t_{direct}$ ) is:

$$t_{direct} = \frac{x}{v}, \quad (1)$$

where  $x$  is the antennae separation and  $v$  is the propagation velocity.

The refracted path of a ray at a boundary is described by Snell's Law (Telford et al., 1990)

$$\frac{\sin i_1}{v_1} = \frac{\sin i_2}{v_2}, \quad (2)$$

where  $i_1$  is the angle of approach from the normal to a boundary in layer 1 (Fig. 1A),  $i_2$  is the angle of refraction from the normal into layer 2, and  $v_1$  and  $v_2$  are the propagation velocities in layers 1 and 2.

A critical refraction is defined as having a refracted angle ( $i_c$ ) of  $90^\circ$ . A critically refracted wave travels from

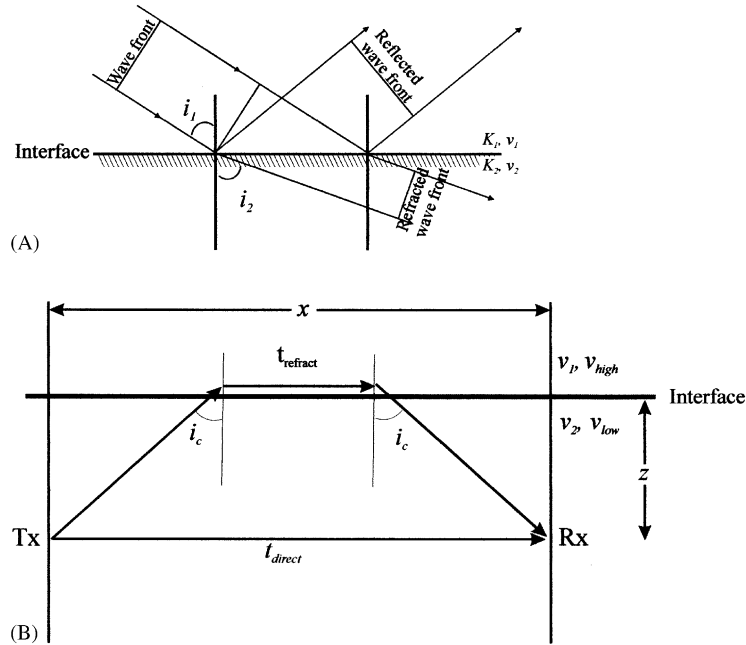


Fig. 1. (A) Ray paths showing direct waves and reflections and refractions at boundary. (B) First arrival travel times measured with borehole ground penetrating radar in zero-offset profiling mode.

the transmitter through the lower-velocity soil to the boundary between the layers of contrasting permittivity at the velocity of the low-velocity medium,  $v_{low}$ . The wave then travels along the boundary at the velocity of the higher velocity medium,  $v_{high}$ . Finally, the wave leaves the boundary at the critical angle and travels to the receiver at  $v_{low}$  (Fig. 1B). A critically refracted wave has a travel time ( $t_{refract}$ ) of

$$t_{refract} = \frac{2z}{v_{low} \cos i_c} + \frac{x - 2z \tan i_c}{v_{high}}, \quad (3)$$

where  $z$  is the vertical distance of the measurement from the boundary between the layers.

The routine MULTLREFRACT was developed to automatically compute the first arrival travel time through an arbitrarily layered soil profile. The spatial structure of ZOP data collection requires that the algorithm assumes that the subsurface is horizontally layered and that each layer is homogeneous and isotropic. For a given propagation velocity profile, the algorithm computes the direct travel time and all possible critically refracted travel times through all of the layers above and below the measurement location. A travel time matrix stores the first arrival travel time data, whereby the direct travel time of layer  $i$  is located at  $(i,i)$  and the refracted travel time through  $j$  layers above and below layer  $i$  is located in columns  $(i,i \pm j)$ . Impossible arrangements of critically refracted travel times, such as the critical refraction from a high-velocity layer into a

low-velocity layer, are given arbitrarily large values (e.g., 99999). The first arrival travel time profile is defined from this matrix as the minimum travel time of each row.

## 2.2. Optimization

Inversion of the velocity profile is ill-posed and nonlinear because the travel path of the first arriving wave depends upon the velocity profile. To overcome this difficulty, a global optimization routine (simulated annealing) was utilized. Simulated annealing is a global search method that searches the parameter space in a controlled random fashion (van Laarhoven, 1988). Similar to physical annealing, where a solid's crystalline structure is controlled by slow cooling in a bath, the energy state of the optimization routine, i.e. its fitness to the measured travel time data, is controlled by decreasing a synthetic temperature through a cooling schedule (Otten and van Ginneken, 1989). A global optimization approach was chosen over a local optimization routine because local methods are known to get trapped in local minima for nonlinear geophysical problems (Boschetti et al., 1996).

The initial velocity profile is calculated assuming that all first arrival times are direct arrivals. This velocity profile is fed to the MULTLREFRACT algorithm and a ray tracing algorithm is used to model the first arrival

travel time profile. If the modeled travel time at a depth is within a travel time misfit allowance ( $t_{allow}$ ) of the measured value, then the arrival is identified as a direct arrival and the velocity is retained. Otherwise, the velocity is assumed to be associated with a critical refraction and the search for the proper velocity profile begins.

The simulated annealing algorithm explores the parameter space through a random walk perturbation of the velocity profile. Specifically, velocity values at depths where the modeled first arrival differs from the measured first arrival by more than  $t_{allow}$  are placed on the stack for perturbation. It is standard practice to measure the travel time above the ground when conducting a survey to calibrate the BGPR response to the known propagation velocity in air. We make use of this known velocity and calculate the velocity profile stepwise from the ground surface downward. A generated random number within a user-defined range is added to the first velocity on the stack. Then the forward model is rerun and the fitness of the solution is re-evaluated. A velocity that lowers the root mean square (RMS) error between the measured and modeled travel time profiles is accepted. A velocity that increases the RMS error is accepted according to a probability distribution dictated by the Metropolis algorithm (Salamon et al., 2002)

$$Pr\{accept_i + 1\} = \begin{cases} 1 & \text{if } E(i+1) \leq E(i), \\ e^{(-\Delta E/c)} & \text{if } E(i+1) > E(i), \end{cases} \quad (4)$$

where  $i$  is the current iteration,  $\Delta E$  is the difference between the new RMS error and the current RMS error,  $c$  is the control parameter, and  $e^{(-\Delta E/c)}$  is the Metropolis criterion. The control parameter is reduced during the course of the simulation following a cooling schedule. A simple cooling schedule is an exponential reduction in the control parameter by

$$c_i = \alpha^i c_0, \quad (5)$$

where  $\alpha$  usually ranges between 0.9 and 0.99 (van Laarhoven, 1988) and  $c_0$  is the initial value of the control parameter. The result of the optimization is the identification of the velocity profile that gives the minimum difference between measured and modeled travel time profiles.

At the beginning of a simulated annealing optimization, the method is similar to the blind random search (Otten and van Ginneken, 1989), where almost every proposed velocity change is accepted. Towards the end of the optimization, the probability of acceptance declines and the method approaches the iterative improvement algorithm (Otten and van Ginneken, 1989). The primary difference is that the iterative improvement algorithm does not accept worse fits to the measured travel time. The value of the control parameter,  $c$ , and the change in RMS error between

iterations,  $\Delta E$ , determines which method the simulated annealing algorithm resembles more closely. For example, a high  $c_i$  and low  $\Delta E$  will cause the Metropolis criterion to be very low. The selection of the newly proposed velocity will occur with high probability, equivalent to the blind random search.

### 2.3. Regularization

Regularization aims to stabilize the solution of an ill-conditioned problem. Ill-conditioning results from the model parameters (velocity) being highly sensitive to the data measurements (travel time). In this application, we use model smoothing to help stabilize the solution. Smoothing is incorporated by minimizing the first and second derivative of the velocity with depth. The minimization of the first derivative aims to reduce the absolute difference between adjacent velocity values. The criterion for applying smoothing is

$$|v_{k+1} - v_{k-1}| < deriv_1, \quad (6)$$

where  $v_{k-1}$  and  $v_{k+1}$  are the velocities of the layers above and below the depth that is undergoing perturbation and  $deriv_1$  is the smoothing factor. If Eq. (6) is exceeded, then the velocity with the largest value is reduced iteratively by 0.01 m/ns for a maximum of 10 iterations. During this iteration procedure, Eq. (6) is checked and iterations stopped if Eq. (6) is met. Similarly, minimization of the second derivative controls the curvature of the profile. Smoothing is applied if

$$|v_{k+1} - 2v_k + v_{k-1}| > deriv_2 \quad (7)$$

where  $deriv_2$  is the controlling parameter for minimization and the absolute value controls positive or negative curvature. The maximum value of  $deriv_2$  is  $2v_{max} - 2v_{min}$  ( $v_{max}$  and  $v_{min}$  are user defined constraints for velocity fitting), which prevents any smoothing. The minimum value of  $deriv_2$  is zero, and forces the three velocities to lie on a straight line.

Controlling the values of  $deriv_1$  and  $deriv_2$  are accomplished through the movement of a single slider bar. The slider bar's value ranges from 0 to  $slide_{max}$ , where  $slide_{max} = (v_{max} - v_{min})$ . Clicking the mouse cursor within the slider bar moves the bar by 10% for each click and clicking on the arrow moves the bar by 1%. To obtain the specific values of  $deriv_1$  and  $deriv_2$  the following equations are used:

$$deriv_1 = slide_{max} \sum percent / 100, \quad (8a)$$

$$deriv_2 = 2slide_{max} \sum percent / 100, \quad (8b)$$

where  $\sum percent$  represents the total percentage change in the slider bar's position dictated by the number and type of clicks performed. Moderate smoothing would be  $deriv_1 = 0.033$  m/ns and  $deriv_2 = 0.066$  m/ns.

We found, through repeated testing, that regularization was necessary to dampen oscillations in the optimized velocity profile. Specifically, without smoothing the fitted velocity profile alternates between extremely high and extremely low velocity values in adjacent layers. Rucker and Ferré (2004b) have shown that such a model could not be observed with ZOP BGPR, because critical refractions in a profile cause the method to act as a low-pass spatial filter. The oscillations occur in the solution when the first velocity on the stack is fit to a value that represents the low end of the uncertainty range in travel time (high velocity). The starting model for the velocity is the direct velocity, which is always higher than any critically refracted velocity. A slow marching away from the direct velocity will always fit toward the higher end. The next velocity to be perturbed, which is most likely an adjacent layer, will have to compensate for the previous layer's fit by fitting towards the opposite end of the travel time misfit. This overcompensation continues down the stack and can be minimized by choosing a smaller  $t_{allow}$ , increase smoothing, or increasing the velocity perturbation value (Rucker and Ferré, 2004a).

#### 2.4. Stochastic parameter estimation

Unlike the direct application of the graphical method, the global optimization approach includes stochastic parameter estimation. That is, the velocity profile is determined repeatedly within the tolerance defined by the time misfit to form a series of Monte Carlo realizations of the water content profile. Inherent errors in travel time measurements prohibit the modeled profile from exactly fitting the measured profile. Therefore, the optimized velocity profile is not unique; many different profiles will fit within the error criterion. Using the principle of ergodicity, it is assumed that each realization has an equal likelihood of being correct. The ensemble statistics of the Monte Carlo simulation are used to characterize the final velocity profile. The mean velocity at each depth is reported as the velocity. Other ensemble statistics of the inferred velocities, including the standard deviation or minimum and maximum fitted velocity within a layer, describe the uncertainty of the velocity.

### 3. Program structure

BGPR\_Reconstruct combines the simulated annealing optimization algorithm with the forward ray tracing model to reconstruct a velocity profile that best fits the measured ZOP BGPR first arrival travel time profile. The program was written within MATLAB version 6 R12, which provides portability among the different computing platforms as well as accessibility for many

practitioners. A graphical user interface (GUI) was used to combine the features of the optimization in a convenient framework.

BGPR\_Reconstruct includes a main processor, a pre-processor, and a post-processor. When calling the program, the first screen the user will see is the main processor (Fig. 2). The main processor is divided into control and display section. The control section allows the user to read in the file containing the travel time data, control the parameters needed for running the optimization routine, and access the pre- and post-processors. The display section plots the travel time and velocity profiles during the iterative global optimization. During each iteration, the plots are updated such that the user can watch the optimization as it approaches a final velocity profile. By watching the optimization progress, the user can gain insight into possible problem areas that would prevent a successful simulation. For example, the travel time misfit allowance may be too restrictive in some layers. This is usually the case when the  $t_{allow}$  is less than the degree of error in the first arrival travel time measurements (Rucker and Ferré, 2004a). Real-time visualization allows a user to catch this and other problems before a large number of realizations are completed. The display section also presents a plot of the RMS error between the modeled and measured travel time profiles as a function of iterations completed.

#### 3.1. Main processor

To begin the inversion, the travel time data are read into the program under the File-Open menu. The travel time data can be in two formats, containing two or three columns. The first column must contain the depths of the measurements, with the first measurement occurring at or above the ground surface. Units for the program are meters for length and nanoseconds for time. For a two-column file, the second column contains the first arrival travel time obtained at each depth from the radargram. For a three-column data file, the second column is the minimum travel time and the third column is the maximum travel time at each depth. This allows a user to define bounding travel times that define the first arriving travel times with a 95% confidence interval. Once opened, the travel time data are plotted.

Default parameter values accompany the BGPR\_Reconstruct program. Parameter values that can be changed are presented in white boxes. All of the other boxes are used to show information only. A slider bar above the velocity profile controls the level of smoothing. The Help menu describes all of the parameters used. After entering the antennae separation, the velocity profile calculated with the assumption that all first arrivals are direct will appear. The Run button starts the optimization algorithm.

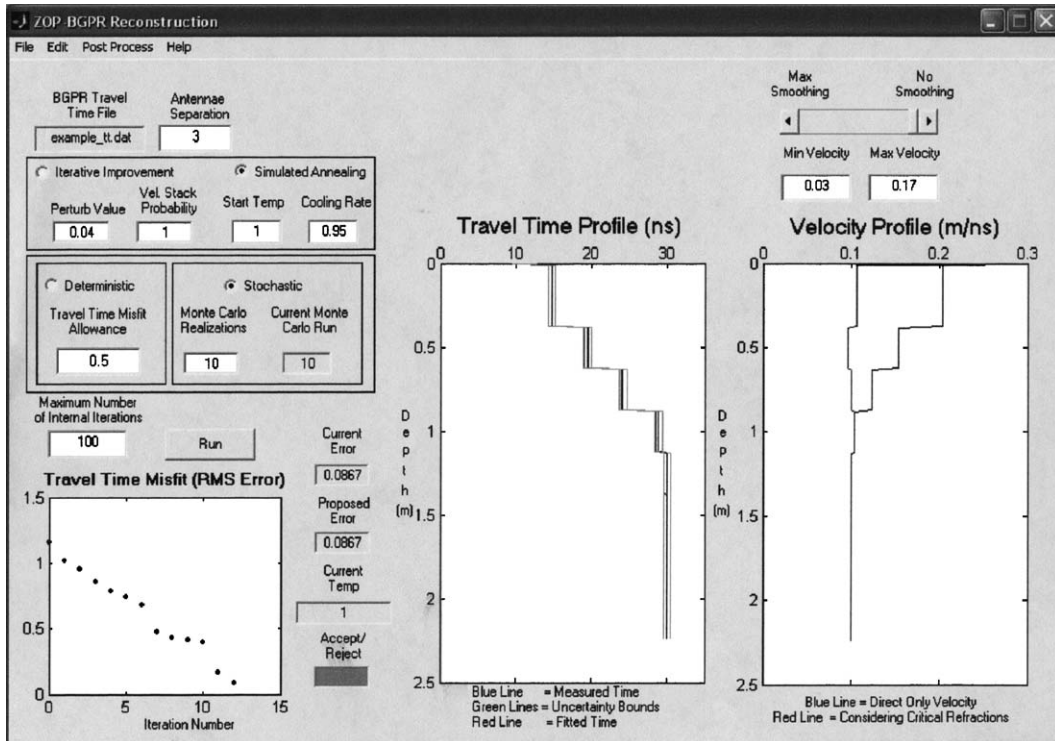


Fig. 2. Main processor screen of BGPR\_Reconstruct, showing travel time profile from homogeneous half-space used in example.

The center blue line on the travel time profile plot represents the measured travel time that the algorithm is trying to fit. The green lines that straddle the blue line represent the travel time misfit allowance or uncertainty range. The blue and green lines stay fixed during simulation. The red line is the modeled travel time. Each layer is perturbed and tested until the red line lies between the green lines at that depth. Once a velocity is accepted, the algorithm moves to the next layer on the stack for perturbation. Because the velocities within every layer can affect the travel path of the first arriving waves in other layers, a layer that has been previously accepted can re-enter the stack when the velocity in another layer is changed. The simulation continues until all velocity values are removed from the stack or when the user-defined maximum number of iterations allowed is exceeded. If the maximum iterations are reached without finding an acceptable velocity profile, the optimization is classified as failed. As the optimization progresses, BGPR\_Reconstruct displays the RMS error between the modeled and measured travel time profiles. The current and accepted errors are displayed in boxes beside the misfit plot.

After the optimization has finished, a log file is placed within the directory. This file lists the accepted RMS error for each iteration of every Monte Carlo realiza-

tion. The user can also save the velocity of each layer for every realization that was successfully completed to a file.

### 3.2. Pre-processor

The pre-processor (Fig. 3) allows the user to change, delete, or add measured first arrival travel time data to the profile. The user can access the pre-processor through Edit-Edit TT File. This function allows users to remove suspect data or to examine the impact of downsampling their data on the inferred velocity profile. In addition, the user can ensure that the first measurement has a velocity that is equal to the velocity of propagation of an EM wave in air by entering the antennae separation and hitting the Adjust button. A plot of travel time shows the original and proposed changed profile. To keep the changes, the OK button is pressed and the user is taken back to the main processor with the adjusted travel time profile.

### 3.3. Post-processor

After completing a Monte Carlo simulation, the velocity data can be converted to water content by choosing the Post Process-Water Content menu

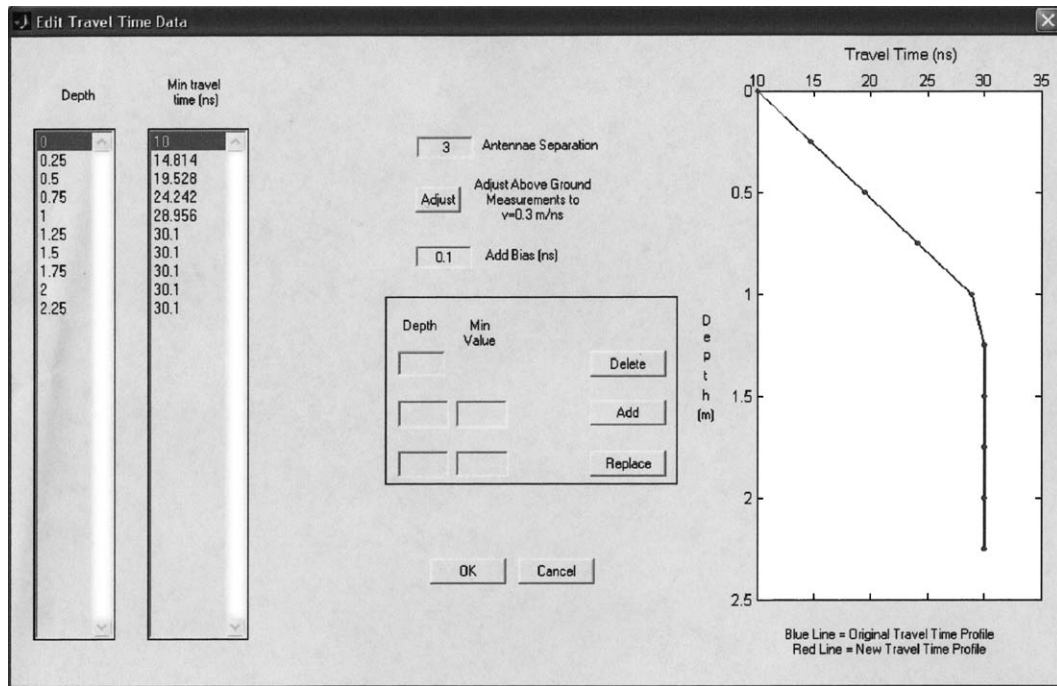


Fig. 3. Pre-processor screen of BGPR\_Reconstruct.

selection. A dialog will be presented (Fig. 4) that plots the ensemble mean of each layer's water content. A user can choose to calculate the water content using the empirical functions of Ferré et al. (1996), Topp et al. (1980), Ledieu et al. (1986), or a user-defined third-order polynomial. The user can also choose the level of uncertainty in water content about the mean to be displayed. The uncertainty is generated from ensemble statistics from the set of Monte Carlo realizations and include the one standard deviation (68% uncertainty), 95% uncertainty, minimum and maximum water content, and others. A separate histogram shows the range and frequency of values for each layer's inferred water content, and the user can choose which layer to display.

#### 4. Example

The following simple example demonstrates the process of inverting a first arrival travel time profile to obtain a water content profile. A more complete discussion of the application of this optimization routine to hydrologic investigations is presented in (Rucker and Ferré, 2004a). Consider a homogeneous half-space. Measurements are made every 0.25 m, starting at 0 m and extending to 2.25 m below ground surface. The subsurface has a constant propagation velocity of 0.1 m/ns, which is characteristic of a mineral soil with a

volumetric water content of  $0.17 \text{ cm}^3/\text{cm}^3$ . Above the ground surface, EM waves propagate at the velocity of light in air, 0.3 m/ns. Above the refraction termination depth of approximately 1 m, critically refracted waves are first to arrive at the receiver (Rucker and Ferré, 2003). Below this depth, direct waves are first arriving. Forward modeled first arriving travel times are plotted with depth in Fig. 2. We assume a travel time measurement uncertainty (travel time misfit allowance) of 0.5 ns to represent both instrument and operator error (Rucker and Ferré, 2004a).

The smoothing criteria of  $deriv_1 = 0.033 \text{ m/ns}$  and  $deriv_2 = 0.067 \text{ m/ns}$  were chosen to minimize the travel time oscillations. Other parameters include a velocity perturbation value of 0.04 m/ns, maximum number of iterations of 100, starting temperature of 1 and cooling rate of 0.95, and 100 Monte Carlo realizations to be performed. The model of Ferré et al. (1996) was used to infer water contents from propagation velocities. All of the 100 realizations were completed successfully. The average number of iterations needed to complete each realization was 22.9. The average final RMS error between the measured and modeled travel time profiles was 0.07 ns. The results of the inferred water content profile are presented in Fig. 4. The ensemble mean water content was approximately  $0.17 \text{ cm}^3/\text{cm}^3$  and one standard deviation in water content is displayed beside the mean in Fig. 4., demonstrating that the optimization

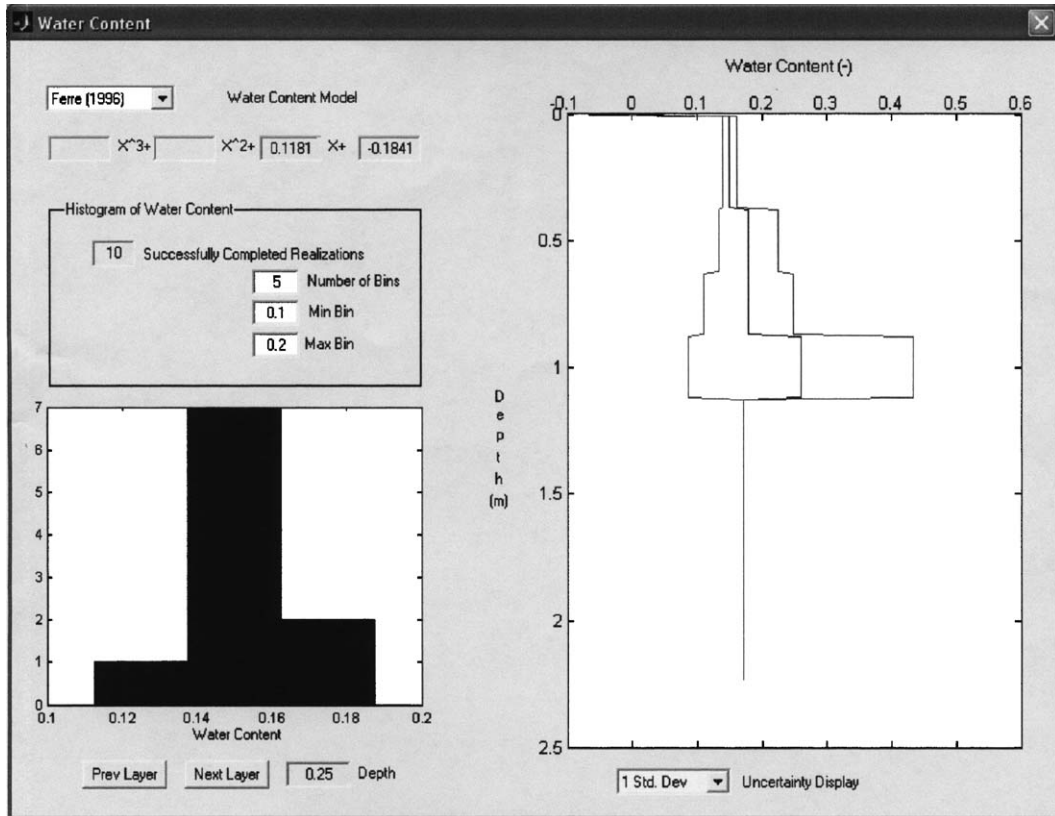


Fig. 4. Post-processor screen of BGPR\_Reconstruct showing example results of inferred water content from 100 realizations.

routine was capable of reproducing the known water content.

As a second example, consider a hypothetical infiltration experiment into the uniform water content profile described above. The water is infiltrated from the surface for 7 h. The top boundary condition is a saturated water content of  $\theta = 0.45$  during the course of the experiment. The analytical solution to a 1-D vertical infiltration with gravity was presented in Warrick et al. (1985). Assuming a silt loam soil with van Genuchten soil hydraulic properties (van Genuchten, 1980) of  $\alpha = 0.01$  ( $\text{cm}^{-1}$ ),  $K_{sat} = 0.006$  ( $\text{cm/s}^1$ ), and  $n = 2$  (dimensionless), the water content profile at 7 h is shown in Fig. 5A. The profile shows a constant water content of 0.45 in the upper 0.6 m, and a gradual decrease to the background water content between 0.6 and 1 m.

The water content profile was converted to a velocity profile using the Ferré model. The ZOP BGPR travel time profile was then constructed with the MULTI-REFRACT algorithm (Fig. 5B). Initially, the water content profile and travel time profile was discretized by 0.05 m. The travel time profile of Fig. 5B was down

sampled to 0.25 m to simulate typical field measurements of ZOP BGPR. The main feature of Fig. 5B is the linear increase in travel time down to 0.75 m, then a linear decrease from 0.75 to 1 m. This is caused by critical refraction with the ground surface in the upper part of the profile giving way immediately to critical refraction at the wetting front. If the higher water content region had been thicker, then a direct arrival would have been seen in the profile with a travel time of 53.6 ns. Because no direct arrival was seen in this high water content region, it is considered a thin layer (Rucker and Ferré, 2004b). Lastly, noise from a uniform distribution was added to the travel time to simulate human error and machine bias in the first break picking of the travel time data (Rucker and Ferré, 2004a).

The inversion of the infiltrated water content profile with added noise can be seen in Fig. 5C. The ensemble mean from 100 realizations is plotted as a solid line and error bars represent the ensemble standard deviation. The BGPR\_Reconstruct parameters for inversion were the same as listed above. Overlain on Fig. 5C is the analytical solution to water infiltrating from the surface. The mean water content profile matches the forward

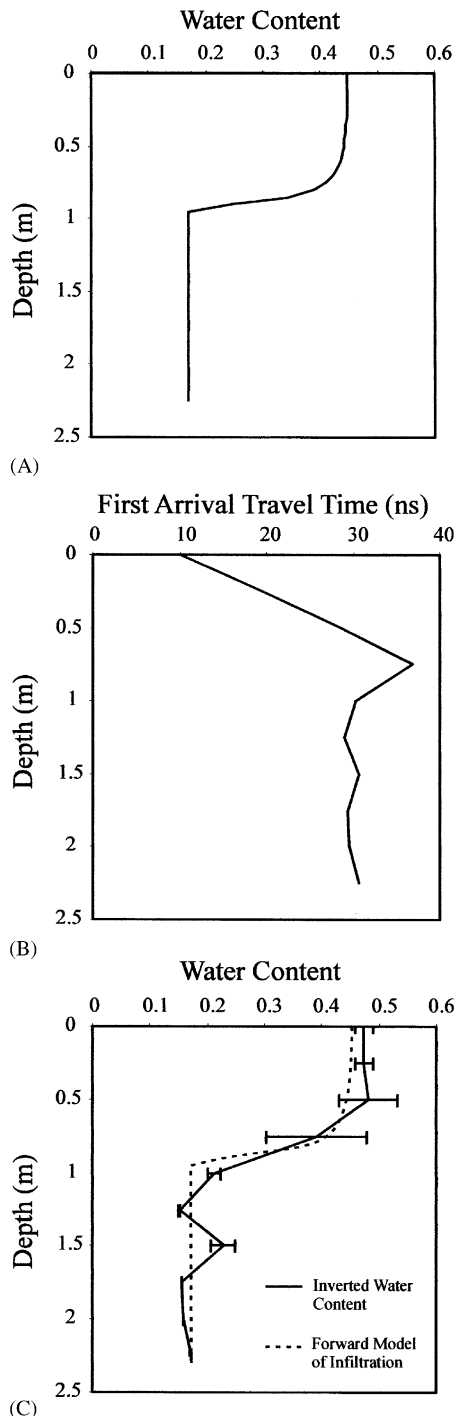


Fig. 5. (A) Analytical forward model of water content profile during infiltration. (B) Travel time profile with noise. (C) Water content profile after inversion of travel time presented in B. Overlain is original forward model.

model quite well. However, there seems to be a large uncertainty about the water content at 0.75 m. This type of uncertainty could be reduced if greater confidence is

placed in the first break pick. Lastly, the water content assuming that the travel path of each measurement was from a direct arrival is shown in Fig. 5C. Even with the large uncertainty at 0.75 m, the automated inversion is a better predictor of the water content than with the purely direct arrival assumption.

## 5. Conclusions

A simulated annealing optimization routine was developed to invert the first arrival travel time profile measured with zero-offset profiling borehole ground penetrating radar. The optimization used a forward ray tracing algorithm and random walk perturbation of the velocity profile to find a velocity profile that minimizes the root mean square error between the modeled and measured travel time profiles. This is an improvement over standard analyses, which do not consider the effects of critical refraction on ZOP BGPR travel time profiles. The routine also presents an improvement over graphical methods in that it can achieve higher vertical resolution of the water content profile while reducing the time and effort required for analysis. In addition, a Monte Carlo simulator is included that allows for the uncertainty in travel time measurements to be incorporated in the inversion, resulting in a measure of the confidence of water content values at each depth in the profile. An example application is shown demonstrating that the routine is capable of inferring the water content profile even at early time during the advance of a wetting front.

The program was developed within the MATLAB environment using a graphical user interface to allow the user to control the optimization parameters needed for successful simulation. The travel time, velocity, and error plots are updated during each iteration, making the solution appear to animate towards the optimal velocity profile. Further background regarding this approach to travel time inversion is provided in (Rucker and Ferré, 2004a).

## Acknowledgements

This material is based on work supported by the National Science Foundation under Grant no. 0097171. Additional support was provided by funds from NASA under Contract NASA/JPL 1236728.

## References

- Boschetti, F., Dentith, M.C., List, R.D., 1996. Inversion of seismic refraction data using genetic algorithms. *Geophysics* 61 (6), 1715–1727.

- Feng, S., Sen, P.N., 1985. Geometrical model of conductive and dielectric properties of partially saturated rocks. *Journal of Applied Physics* 58 (8), 3236–3243.
- Ferré, P.A., Rudolph, D.L., Kachanoski, R.G., 1996. Spatial averaging of water content by time domain reflectometry: implications for twin rod probes with and without dielectric coatings. *Water Resources Research* 32 (2), 271–279.
- Friedman, S.P., 1997. Statistical mixing model for the apparent dielectric permittivity constant of unsaturated porous media. *Journal of Hydrology* 61, 742–745.
- Friedman, S.P., 1998. A saturation degree-dependent composite spheres model for describing the effective dielectric constant of unsaturated porous media. *Water Resources Research* 34 (11), 2949–2961.
- Ledieu, J., de Ridder, P., de Clark, P., Dautrebande, S., 1986. A method of measuring soil moisture by time-domain reflectometry. *Journal of Hydrology* 88, 319–328.
- Otten, R.H.J.M., van Ginneken, L.P.P.P., 1989. *The Annealing Algorithm*. Kluwer Academic Publishers, Dordrecht, The Netherlands, 201pp.
- Rucker, D.F., Ferré, T.P.A., 2003. Near-surface water content estimation with borehole ground penetrating radar using critically refracted waves. *Vadose Zone Journal* 2 (2), 247–252.
- Rucker, D.F., Ferré, T.P.A., 2004a. Automated water content reconstruction of zero-offset borehole ground penetrating radar data using simulated annealing. *Water Resources Research*, submitted for publication.
- Rucker, D.F., Ferré, T.P.A., 2004b. Correcting water content measurement errors associated with critically refracted first arrivals on zero offset profiling borehole ground penetrating radar profiles. *Vadose Zone Journal* 3 (1), 278–287.
- Salamon, P., Sibani, P., Frost, R., 2002. *Facts, Conjectures, and Improvements for Simulated Annealing*. SIAM, Society for Industrial and Applied Mathematics, Philadelphia, PA, 150pp.
- Tabbagh, A., Camerlynck, C., Cosenza, P., 2000. Numerical modeling for investigating the physical meaning of the relationship between relative dielectric permittivity and water content in soils. *Journal of Hydrology* 36 (9), 2771–2775.
- Telford, W.M., Geldart, L.P., Sheriff, R.E., 1990. *Applied Geophysics*. 2nd Edition, Cambridge University Press, New York, NY, 770pp.
- Topp, G.C., Davis, J.L., Annan, A.P., 1980. Electromagnetic determination of soil water content: measurements in coaxial transmission lines. *Water Resources Research* 16 (3), 574–582.
- van Genuchten, M.Th., 1980. A closed-form equation for predicting the hydraulic conductivity of unsaturated soils. *Soil Science Society of America Journal* 44, 892–898.
- van Laarhoven, P.J.M., 1988. *Theoretical and Computational Aspects of Simulated Annealing*. Stichting Mathematisch Centrum, Centrum voor Wiskunde en Informatica, Amsterdam, 168pp.
- Warrick, A.W., Lomen, D.O., Yates, S.R., 1985. A generalized solution to infiltration. *Soil Science Society of America Journal* 49 (1), 34–38.